MSc in Photonics

PHOTONICS**BCN**

Universitat Politècnica de Catalunya (UPC)
Universitat Autònoma de Barcelona (UAB)
Universitat de Barcelona (UB)
Institut de Ciències Fotòniques (ICFO)

http://www.photonicsbcn.eu

Master in Photonics

MASTER THESIS WORK

Preparation of entangled Dicke states using atomic ensembles

Albert Franquet González

Supervised by Dr. Darrick E. Chang, (ICFO)

Presented on date 9th September 2013

Registered at

Escola Tècnica Superior d'Enginyeria de Telecomunicació de Barcelona

Preparation of entangled Dicke states using atomic ensembles

A. Franquet

ICFO-Institut de Ciències Fotòniques, Mediterranean Technology Park, 08860 Castelldefels, Barcelona, Spain

E-mail: Albert.Franquet@icfo.es

Abstract. Phenomena associated with collective interactions in atom-nanofiber interfaces have been of great interest. Here, we show how multipartite entanglement in atomic ensembles can emerge from collective emission in combination with photon detection. We present a novel group theoretical technique to efficiently calculate the dynamics of this many-body system.

Keywords: Atom-nanofiber interface, Dicke States, Entanglement, Decoherence, Quantum Open Systems, Quantum Master Equations.

1. Introduction

Controlling and interfacing light with atoms is the basic ingredient for many applications in quantum information science [1]. Photons are convenient to carry information over large quantum networks, while atoms naturally produce and interact with single photons. This promising atom-light interface developed in recent years consists of cold atoms trapped near tapered nanofibers [2, 3]. These hybrid systems are well characterized and have been proven to enable $\sim 1-10\%$ coupling efficiencies of a single atom to the fiber. Although this single-atom coupling might be relatively weak, there exist collective modes of a trapped atomic ensemble whose coupling to light is enhanced by the square root of the atom number, $\sqrt{N}$ [4]. It has been shown that collective enhancement yields new interesting phenomena such as atomic Bragg mirrors or self-organization [5, 6].

This new scenario interfacing atoms with nanophotonics provides a way to engineer infinite-range interactions between atoms, this can be qualitatively understood by recalling that a photon emitted by one atom into the fiber can propagate without attenuation until it scatters off a second atom. Making it a good candidate to produce and manipulate many-body entangled atomic states at once by just letting the system evolve from a symmetrical excited initial state. In contrast, entanglement is usually obtained from a product of multiple 2-body interactions, which makes it difficult to scale up.

In this work we examine the dynamics of the atomic ensemble in this hybrid nanofiber system where atoms can experience infinite-range dipole-dipole photon mediated interactions. The whole dynamics of the atomic ensemble are controlled by a collective decay coupled to the nanofiber and independent spontaneous decay to free space. We show how quantum correlations and entanglement are created and destroyed in the system through collective and individual decay of the atomic ensemble when starting

in a fully excited initial state of the ensemble. In this context, the density matrix evolution can be fully computed using a novel SU(4) group theory technique [7] to overcome the inefficiency of the Dicke basis naturally used in the literature. It is shown that although the pure basis states are known to have genuine multipartite entanglement, the incoherently evolved mixed states cannot be said to have genuine multipartite entanglement without ambiguity. Nevertheless, a trick to counter it using single-photon detection is presented, which improves the scaling with the number of atoms by $\sqrt{N}$ and permits to create up to $N \sim 10$-atom genuine multipartite entangled Dicke states in the more restrictive superradiant regime [8, 9].

2. Atom-nanofiber interface model and its spin-spin dynamics formulation

The coupling of laser-cooled atoms with light by means of tapered optical nanofibers has been an active field of research over the past years. In this case, the atoms remain at the outside of a fiber and couple to the evanescent field surrounding the fiber. Up to $N \sim 10^3$ atoms have been loaded from a magneto-optical trap (MOT) into a two-color optical dipole trap, which makes use of a red- and blue-detuned evanescent light field around the optical nanofiber [2]. Figure 1 shows on the left, the described system

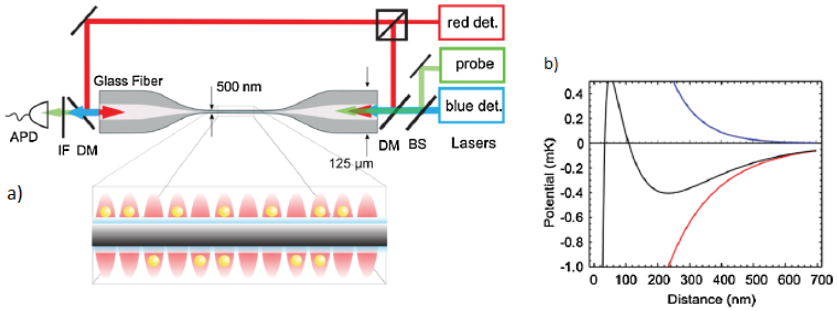

Figure 1. The experimental set-up used in [2] is depicted on the top left corner. Figure a) shows the lattice potential created in the nanowaveguide region where the atoms are trapped. Figure b) shows the effective trapping potential seen by a cesium atom in the evanescent field region versus the distance from the nanowaveguide.

and on the right, the potential calculated for a ground state cesium atom subjected to such a two-color evanescent light field around a 500-nm diameter nanofiber.

Our system is modelled as an ensemble of N two-level atoms with ground and excited states $|g\rangle$, $|e\rangle$ and resonance frequency ω_A located at positions z_j. The atoms are interacting with a one-dimensional nanofiber supporting left- and right-propagating fields $a_{L,R}$, $a^\dagger_{L,R}$ with velocity v through a dipole coupling. Yielding a full Hamiltonian containing atoms, fields and interaction of the form:

$$\begin{aligned} H = &\sum_{j=1}^{N} \hbar w_0 \sigma_{ee}^j + \mathrm{i}\hbar v \int \mathrm{d}z \left(a_L^\dagger \frac{\partial a_L}{\partial z} - a_R^\dagger \frac{\partial a_R}{\partial z} \right) \\ &-\hbar g \sqrt{2\pi} \int \mathrm{d}z \sum_{j=1}^{N} \delta(z - z_j) \left(\sigma_{eg}^j (a_R(z) + a_L(z)) + \mathrm{h.c.} \right) \end{aligned} \tag{1}$$

where $\sigma_{eg}^j = |e\rangle\langle g|_j$ are the atomic coherence operators and $a_{L,R}$, $a^\dagger_{L,R}$ are the left and right going field mode annihilation and creation operators fulfilling the usual commutation relations $[a_{L,R}(z), a^\dagger_{L,R}(z')] = \delta_{L,R}\delta(z - z')$ and with g being the dipole

coupling strength. The independent decay of the atomic cloud into modes outside of the waveguide is introduced as a Lindblad decay contribution onto the density matrix evolution of the form:

$$\mathcal{L}[\rho] = -\frac{\gamma}{2}\sum_{j=1}^{N}\left(\{\sigma_{eg}^{j}\sigma_{ge}^{j},\rho\} - 2\sigma_{ge}^{j}\rho\sigma_{eg}^{j}\right). \tag{2}$$

From the Hamiltonian (1), one can compute the Heisenberg equations of motion for the atomic coherences and get the single-atom spontaneous emission rate into the waveguide $\Gamma_{1D} = 4\pi g^2/v$. Further simplification results if the atomic coherences are slowly varying, $\sigma_{ge}^{j}(t-\epsilon) \approx \sigma_{ge}^{j}(t)\mathrm{e}^{\mathrm{i}\omega_A\epsilon}$, and if the characteristic bandwidth $\Delta\omega$ of the dynamics satisfies $\Delta\omega L/v \ll 1$, where L is the system length. In this limit, the photon-mediated dipole-dipole interactions between atoms are described by a master equation $\dot{\rho} = -\mathrm{i}[H_{dd},\rho] + \mathcal{L}_{dd}[\rho]$ for the atomic density matrix ρ, where

$$H_{dd} = \frac{\Gamma_{1D}}{2}\sum_{j,k}\sin(k_A|z_j - z_k|)\sigma_{eg}^{j}\sigma_{ge}^{k} \tag{3}$$

and

$$\mathcal{L}_{dd}[\rho] = -\frac{\Gamma_{1D}}{2}\sum_{j,k}\cos(k_A|z_j - z_k|)\left(\{\sigma_{eg}^{j}\sigma_{ge}^{k},\rho\} - 2\sigma_{ge}^{k}\rho\sigma_{eg}^{j}\right). \tag{4}$$

Here the energy difference between $|g\rangle$ and $|e\rangle$ is eliminated as it will not play a role in the dynamics given that all the atoms are equal and already coupled to the fiber, $k_A = 2\pi/\lambda_A$ is the resonant wavevector and the sum on j, k runs over all atoms. The Hamiltonian (3) characterizes the field-mediated dipole exchange between atoms, while the incoherent evolution $\mathcal{L}_{dd}$ characterizes cooperative emission. Remarkably, the interactions are infinite in range and sinusoidal, since a photon emitted by one atom into the fiber propagates without attenuation until it scatters off a second atom, and the interaction should be sensitive only to the relative phases between them.
An additional contribution to the density matrix evolution $\mathcal{L}[\rho]$ with the form of (2) characterizes independent atomic emission into free space at a rate γ.
An effective three level structure for the atoms and a pump laser of strength Ω to couple some transition is depicted in Fig. 2.

Using the Schrieffer-Wolff transformation, one can adiabatically eliminate the level e

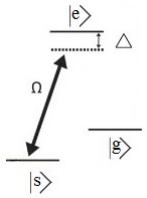

Figure 2. Scheme of a possible three-level atom configuration. An auxiliary state $|s\rangle$ is used to tune the decay rate to the ground state $|g\rangle$ by coupling the former excited state $|e\rangle$ to the auxiliary state with a pump laser of strength Ω tunable in time. The detuning between the pump laser Ω and the state energy difference of $|s\rangle$ and $|e\rangle$ is Δ.

and the evolution will take place with the new effective excited level s making now the coupling between g and s tunable by the pump laser. Now the interaction Hamiltonian (3) and the Lindblad collective decay (4) are changed accordingly to

$$H_{dd} \approx \frac{\Omega(t)^2}{2\Delta^2}\Gamma_{1D}\sum_{j,k}\sin(k_A|z_j - z_k|)\sigma_{sg}^{j}\sigma_{gs}^{k}$$

and

$$\mathcal{L}_{dd}[\rho] \approx -\frac{\Omega(t)^2}{2\Delta^2}\Gamma_{1D}\sum_{j,k}\cos(k_A|z_j - z_k|)\left(\{\sigma_{sg}^{j}\sigma_{gs}^{k},\rho\} - 2\sigma_{gs}^{k}\rho\sigma_{sg}^{j}\right).$$

With the advantage that now the decay rate $\frac{\Omega(t)^2}{2\Delta^2}\Gamma_{1D}$ is tunable in time by the pump laser, i.e., one can stop the evolution when desired.
As the equations (3) and (4) are only changed in the rates, for simplicity we will keep the same formulation of the model as a two-level system for the present work.
We will focus on a particular scenario where the atoms are spaced by integer multiples of λ_A. In that case, the Hermitian field-mediated dipole exchange between atoms (3) vanishes and the incoherent evolution of the atomic density matrix is:

$$\dot{\rho} = \mathcal{L}_{dd}[\rho] + \mathcal{L}[\rho] \tag{5}$$

with

$$\mathcal{L}_{dd}[\rho] = -\frac{\Gamma_{1D}}{2}\left(\{J^+J^-,\rho\} - 2J^-\rho J^+\right). \tag{6}$$

and $\mathcal{L}[\rho]$ being (2). $J^+ = \sum_{j=1}^{N}\sigma_{eg}^j$ and $J^- = \sum_{j=1}^{N}\sigma_{ge}^j$ are the ladder operators of the total angular momentum representation of the spins (atoms). The coupling of the atoms with the fiber mode becomes a collective atomic decay into the waveguide (6) while the spontaneous emission into free space is an individual decay term (2).
In general, for all but smallest values of N, exact analytic solutions to equation (5) are intractable, and it is necessary to resort to numerical simulation approaches such as the quantum trajectory method or quantum Monte Carlo. Even so, treating more than 10 spins is difficult due to the restriction imposed by the 2^N scaling of the Hilbert space dimension with the number of atoms. However, due to the symmetry of the master equation, the atomic density matrix evolution will take place in a reduced subspace of dimensionality $\sim N^2$.

Basis states

The invariance of the master equation (5) under arbitrary permutation of the atoms makes convenient to describe the system using the Dicke basis, which is shown on the top left-hand-side in Fig. 3. Here M is the $J_z = \frac{1}{2}\sum_{j=1}^{N}(\sigma_{ee}^j - \sigma_{gg}^j)$ eigenvalue and J is the $J^2 = J^-J^+ + J_z^2 + J_z$ eigenvalue as usual. The total number of Dicke states is 2^N, which is the dimension of the full Hilbert space. However, for describing the process of interest, it is sufficient to use a smaller set of orthonormal states shown on the top right-hand-side of Fig. 3. Specifically, in [10] it is shown that the transition probabilities between these states do not depend on the degeneracy of a specific $\{J, M\}$ subspace, meaning that we can reduce the basis dimension taking any of the degenerate column subspaces for each $\{J, M\}$ set as all the other columns in the set will be exact copies for describing the process of interest.

In the new basis states, the Γ_{1D} decay has a simple form (see Fig. 3): it goes only downwards, and the decay rate from state $|J, M\rangle \to |J, M-1\rangle$ is given by the usual Dicke formula $\Gamma_{1D}(J+M)(J-M+1)$.
Unfortunately, γ decay does not look simple. It can be shown (using addition rules for angular momentum) that $|J, M\rangle$ couples only to $\{|J+1, M-1\rangle, |J, M-1\rangle, |J-1, M-1\rangle\}$ states due to the symmetry rules of the SU(2) algebra (see Fig. 3). This occurs with a decay rate proportional to the number of excited atoms n_e.
The evolution imposed by the master equation (5) on the atomic density matrix can then be converted into a classical rate equation redistributing population between the basis states given that one can calculate the Γ_{1D} and γ rates efficiently,

$$\langle J, M|\dot{\rho}|J', M'\rangle = \langle J, M|\left(\mathcal{L}_{dd}[\rho] + \mathcal{L}[\rho]\right)|J', M'\rangle. \tag{7}$$

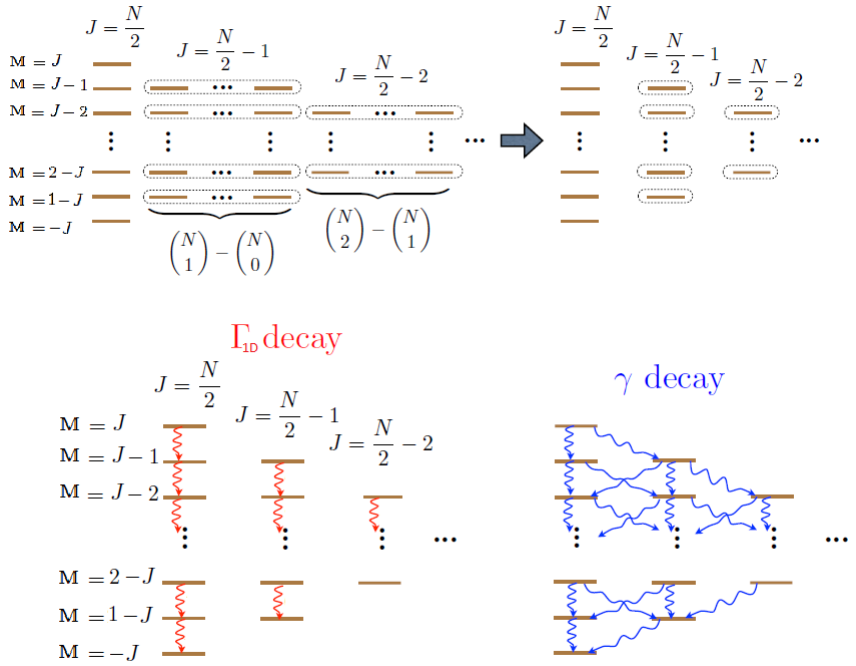

Figure 3. In the case of complete permutation symmetry the complete set of 2^N Dicke states (top-left) can be simplified into a much smaller $\mathcal{O}(N^2)$ set of states (top-right). In the reduced symmetrical basis, Γ_{1D} collective decay is simple, while individual γ decay is complicated (bottom)

The Dicke state picture is not only interesting because it provides an easy way to understand the physical process of the atomic ensemble evolution, but also because the symmetrical nature of Dicke states provides them with nice characteristics from the Quantum Information point of view [11].
All Dicke states but the $|J = N/2, M = \pm N/2\rangle$ extreme states are highly entangled. For example, the $|J = N/2, M = 0\rangle$ state for even N exhibits N-particle genuine multipartite entanglement, i.e., it is entangled with respect to all bipartitions. A lot of features on entanglement have been studied for Dicke states, e.g., the effect of noise [12] or its remarkable robustness to particle loss (it has been proven that $|J = N/2, M = -N/2+1\rangle$ optimizes the concurrence when all but two spins have been removed [13]). These properties make Dicke states an interesting class of multipartite entangled states for experimental examination of genuine multipartite entanglement and important applications in quantum information.

3. Dynamics and results

Due to all of these features, we will examine the possibility of using such a system to create highly entangled Dicke states by letting the trapped atomic ensemble decay freely from an initial totally excited state ($|N/2, N/2\rangle = |e, e, ..., e\rangle_N$). We will simulate dynamics for quite a large amount of atoms and measure the entanglement during the cascade down the ladder of Dicke states.

Entanglement measurement criteria

To quantify the amount of entanglement, we use different entanglement measures based in both bounds in observable values and variances, and fidelity-based

entanglement criterion. From the first kind, we will use one measure to detect entanglement in the vicinity of symmetric Dicke sates [14]. From the second kind, we will measure the overlap of our atomic state with a highly entangled state as $|J = N/2, M = 0\rangle$ to be greater than some bound (we consider even N here).
The first kind of measure is more desirable in the experimental realisation because it only relies on the expected values of collective observables, and thus, individual addressing of the atoms is not needed. Also, it is basically a bound on the emitted light intensity [9].
Criterion 1: For separable states,

$$\langle J_x^2\rangle + \langle J_y^2\rangle \leq \frac{N}{2}\left(\frac{N}{2}+\frac{1}{2}\right). \tag{8}$$

Any state violating this condition is confirmed to be entangled.
Criterion 2: For biseparable quantum states ρ,

$$Tr[\rho|N/2,0\rangle\langle N/2,0|] \leq \frac{1}{2}\frac{N}{N-1} =: C_{N/2,0}, \tag{9}$$

where $C_{N/2,0}$ is the square of the maximal overlap of $|N/2,0\rangle$ with biseparable states.

Superradiant regime

We first examine an ideal regime in which the collective decay through the waveguide dominates, i.e., $\Gamma_{1D} >> \gamma$. In this parameter regime, the master equation (5) reduces to the superradiant equation (6) [9]. In that case, all the dynamics occur in the reduced subspace of the $N+1$ maximally symmetric Dicke states (first column of maximal $J = N/2$ in Fig. 3). Then all the evolution can be described by a classical rate equation for the probabilities $P_M(t)$ of being in state $|J = N/2, M\rangle$,

$$\frac{\mathrm{d}P_M(t)}{\mathrm{d}t} = -\Gamma_{1D}(J+M)(J-M+1)P_M + \Gamma_{1D}(J-M)(J+M+1)P_{M+1}. \tag{10}$$

Integration of equation (10) will give the atomic density matrix $\rho(t) = \sum_{M=-J}^{J} P_M(t)|J,M\rangle\langle J,M|$ at any time t. Recalling that *Criterion 2* will simply be the comparison of $P_{M=0}(t) = Tr[\rho(t)|J,0\rangle\langle J,0|]$ with the bound in (9) one can make already some observations.
In Fig. 4 we plot the population distribution of the atomic density matrix for some times during the evolution (big plot) and the scaling of the maximum population of the target $|J,0\rangle$ state achieved during the cascade with the number atoms N (small center plot). $P_M(t)$ starts at $t = 0$ from the $\delta_{J,M}$ Dirac distribution and spreads out very quickly over a wide range of M values as the system cascades down. At early times, $P_M(t)$ has an exponentially decreasing shape. At later times, when the average $\langle M\rangle$ value gets close to zero (point of half emission), $P_M(t)$ is a bell-shaped distribution practically covering all M values. At still later times, towards the end of the cascade, $P_M(t)$ gets narrower and ends up as the $\delta_{-J,M}$ Dirac distribution (for infinite time). The fact that $P_M(t)$ is, in the middle of the emission process, a wide distribution over M values is due to the strong and fast build up of correlations between the atomic atoms, and has a purely quantum origin, the reason being starting the evolution from a state of maximum symmetry between any atom.
Consequently, the absolute value for the probability of finding the atomic ensemble in a entangled state such as $|J,0\rangle$ is extremely small, showing a $\sim N^{-1}$ scaling for its maximum value (center plot in Fig. 4), and the bound in *Criterion 2* (eq. (9)) will

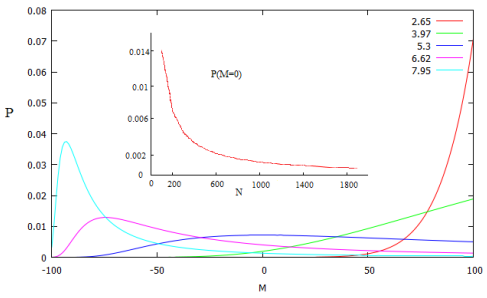

Figure 4. The big plot shows the population of the $N+1$ Dicke states during the superradiant cascade for an atomic ensemble of $N = 200$ atoms. Each curve corresponds to a different time in units of $(N\Gamma_{1D})^{-1}$ during the evolution (evolution from right to left). Note the evolution of the distribution which is narrow at small time (red curve) broadens to cover the whole range of M values at intermediate times (green, blue and purple curves) and becomes narrow again at the end (cian curve) of the evolution. In the small center plot the maximum population of the $|J,0\rangle$ during the whole evolution scaling with the number of atoms N is plotted, revealing a $\sim N^{-1}$ behaviour.

never be reached.

Nevertheless, one can try to improve the method by taking out information of the ensemble during the evolution. This can be achieved by single-photon detections in the waveguide, which can be experimentally conceived by placing single-photon detectors at the ends of the waveguide with no need of separate addressing of different atoms (as already proposed in [15]).

We model the detectors with a single-photon detection efficiency $0 \leq \eta \leq 1$. Then, if one record m detections the atomic density matrix is conditioned accordingly and collapses to a new density matrix

$$\tilde{\rho}_m(t) = \frac{\sum_{i=0}^{N-m} \binom{m+i}{m} \eta^m (1-\eta)^i P_{J-m-i}(t) |J, J-m-i\rangle\langle J, J-m-i|}{Tr[\sum_{i=0}^{N-m} \binom{m+i}{m} \eta^m (1-\eta)^i P_{J-m-i}(t) |J, J-m-i\rangle\langle J, J-m-i|]}. \quad (11)$$

The effect of photon detections on the density matrix is to shrink the subspace of sates where the evolution takes place. For example, if one makes a photon detection, then it is impossible to find the atomic ensemble in the totally excited state $|N/2, N/2\rangle$ because at least one atom has been de-excited. That is what equation (11) is exactly accounting for. It accounts for the possibility of m detections for $m+i$ emitted photons, that is, with the atomic ensemble in the state $|J, J-m-i\rangle$. Clearly, with perfect detection, $N/2$ detection events deterministically produces $|N/2, 0\rangle$.

In general, the probability of finding the atomic ensemble in the $|J,0\rangle$ middle state at time t after having recorded m photon detections with efficiency η (i.e., the population of $|J,0\rangle$ state) is:

$$\tilde{P}_0(t,m) = \frac{P_0(t)\binom{J}{m}\eta^m(1-\eta)^{J-m}}{Tr[\sum_{i=0}^{N-m} \binom{m+i}{m} \eta^m (1-\eta)^i P_{J-m-i}(t) |J, J-m-i\rangle\langle J, J-m-i|]}. \quad (12)$$

With this new strategy of photon detections one could find a combination of parameters, such as time t of evolution, m detection recordings and detector efficiency η, for which it is confirmed that the atomic ensemble exhibits genuine multipartite entanglement for a considerable amount of atoms (states of around $N \sim 10$ atoms are achievable).

Figure 5 gathers all these features. There are two separate regions in the plot, separated by the *Criterion 2* bound for genuine multipartite entanglement (purple curve), a purple region where the state is confirmed to be genuine N-partite entangled and a grey region where the state is biseparable (separable at least by one partition). The black curve shows the maximum $|J,0\rangle$ state population scaling with the number of atoms N if no photon-detection strategy is used (as in the center plot of Fig. 4)

during the evolution, which is not entangled as described earlier. The blue, green and red curves are respectively the $|J,0\rangle$ state population (12) scaling with the number of atoms N when it is optimized in terms of the time t of the evolution and the number m of single-photon detections for detection efficiencies of $\eta = 0.9, 0.8, 0.7$.
Thus, there will be a time t during the evolution for which, when a convenient number of single-photon detections m is recorded, having enough efficiency in these detections ($\eta \sim 0.9$) will be sufficient to experimentally confirm the atomic density matrix to be in a genuine $N \sim 10$-atom entangled state. And it is confirmed (right plot) a $\sqrt{N}$ improvement in the scaling when using this strategy.

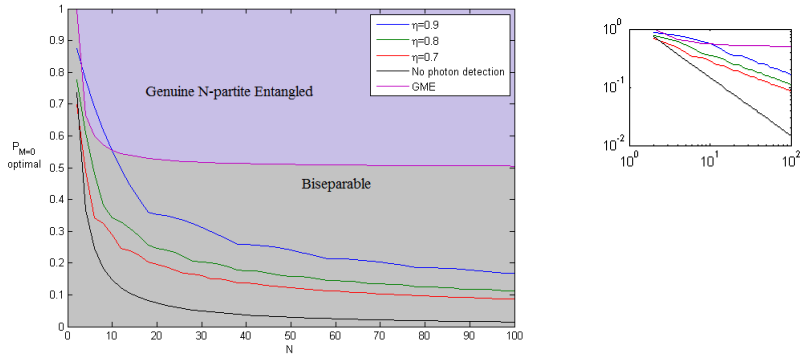

Figure 5. The scaling of the middle state $|J,0\rangle$ population with the number of atoms is computed now for the photon-detection conditioned atomic density matrix (12)(left plot), showing a parameter regime where the atomic density matrix is confirmed to have genuine multipartite entanglement for up to $N \sim 10$ atoms (crossing of blue curve with purple curve). The scaling is also improved by a factor of $\sqrt{N}$ (blue, green and red curves) with respect to the superradiant decay alone (black curve) as depicted in the right plot, which is the same as the left plot but in logarithmic scale.

Competition between collective and non-collective decay

We should now focus our attention on a more realistic scenario when there is some independent atomic decay with spontaneous emission to free space at a rate $\gamma \sim \Gamma_{1D}$. In that case, one should expect that while the collective atomic decay rapidly builds up entanglement between the trapped atoms, the non-collective decay into free space emission will destroy the atomic states symmetry and entanglement. This can be qualitatively understood by noting that the non-collective decay is effectively labelling one particular atom outside of the Dicke state, and thus, it is forcing a new partition of the state ($|J,M\rangle_N \rightarrow_\gamma |J-1/2, M-1/2\rangle_{N-1} \otimes |g\rangle_1$).
As said before, we use a novel technique to efficiently simulate the master equation (5). This new theoretical approach is explained and detailed in the supplementary material of [7], but we will give an intuitive explanation.
Producing an eigenstate basis to diagonalize in general any master equation in the Lindblad form is the aim of this technique. It is based on the construction of an SU(4) algebra defined by 18 super-operators (15 of which are independent), and they are defined forming also six SU(2) subalgebras (like the usual angular momentum algebra). Then one can define basis "states"‡ from the fundamental representation of the SU(4) group adapted to serve as basis of the single-spin density matrix, given by

‡ These states span the density matrix rather than the Hilbert space, so here the word state does not have the same physical sense as before.

$u = |e\rangle\langle e|$, $d = |g\rangle\langle g|$, $s = |e\rangle\langle g|$, $c = |g\rangle\langle e|$. For our symmetrical case the basis is defined as

$$P^s_{q,q_3,\sigma_3} = \mathcal{S}(u^\alpha d^\beta s^\xi c^\delta), \tag{13}$$

where $\mathcal{S}$ is a symmetizer and of course $\alpha+\beta+\xi+\delta = N$. And requiring them to be eigenstates of both $\mathcal{O}^2$ and $\mathcal{O}_3$, with eigenvalues

$$\mathcal{O}^2 P^s_{q,q_3,\sigma_3} = o(o+1)P^s_{q,q_3,\sigma_3}, \quad \mathcal{O}_3 P^s_{q,q_3,\sigma_3} = o_3 P^s_{q,q_3,\sigma_3}$$

where $\mathcal{O}$ is any of these 18 super-operators. The eigenvalues q, q_3, σ_3 are taken to label the basis states for convenience, because in terms of $\alpha, \beta, \xi, \delta$ they are

$$q = (\alpha+\beta)/2, \quad q_3 = (\alpha-\beta)/2, \quad \sigma = N/2 - q, \quad \sigma_3 = (\xi-\delta)/2. \tag{14}$$

Recall that for our initial state $q = N/2, q_3 = N/2, \sigma_3 = 0$, i.e., $P^s_{N/2,N/2,0} = |N/2,N/2\rangle\langle N/2,N/2|$, and also that the master equation (5) is σ_3 conserving because the jump terms act coherently from the left and from the right (keeping $\xi = \delta$). Then, rewriting the master equation using these 18 super-operators, it can be transformed into a new rate equation for the $P^s_{q,q_3,\sigma_3=0}$ states. Redistributing the atomic population starting from $P^s_{N/2,N/2,0}$ state, and coupling $\{q, q_3\} \to \{q\pm1, q_3\pm1\}$ states. Then, the atomic density matrix is described by $\rho = \sum_{q,q_3} C_{q,q_3} P_{q,q_3}$ (as $\sigma_3 = 0$ at all times) with $q = 0, 1, 2, ..., N/2$ and $q_3 = -q, -q+1, ..., q-1, q$ for even N or $q = 1/2, 3/2, ..., N/3$ for odd N. The resulting computational complexity thus scales like $\sim N^2$

In fact, the q_3 eigenvalue is exactly the M eigenvalue in the Dicke state picture (Fig. 3) and the q eigenvalue is, in some sense, quantifying the symmetry as J does for the Dicke states.

One can also map this SU(4) basis again to the Dicke basis making use of a systematic algorithm as pointed out in [7] in order to calculate some observables that can be difficult to implement in the SU(4) picture.

With all this machinery we simulate again the evolution of the density matrix but now for a realistic regime in which the non-collective decay γ is not negligible.

In Fig. 6 we depict the atomic density matrix evolution through the Dicke basis states for $N = 3$ atoms and a ratio of $\Gamma_{1D}/\gamma = 0.1$ (Purcell Factor) to show how the γ decay is now coupling effectively states with different symmetry J as depicted previously in Fig. 3.

In Fig. 7 we plot the scaling for the optimal value of the entanglement measure of

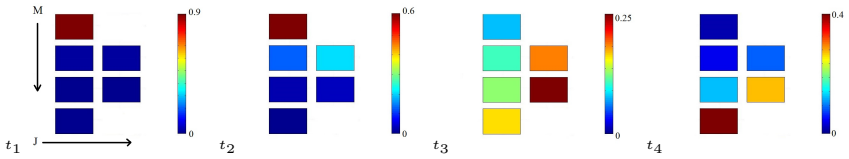

Figure 6. The population of the atomic Dicke sates is depicted for different times of the evolution ($t_1 < t_2 < t_3 < t_4$) for the $N = 3$ atoms case with $\Gamma_{1D}/\gamma = 0.1$. Now the γ decay efficiently populates the $J = 1/2$ states during the evolution but also populating almost every state at middle times t_3.

Criterion 1: $\langle J_x^2\rangle + \langle J_y^2\rangle$ with the number of atoms N for up to $N = 20$ atoms in a regime of $\Gamma_{1D}/\gamma = 0.1$ optimized in time. There are two distinct regions in the plot which are separated by the bound in *Criterion 1* (eq. (8)), a green region where the system is confirmed to be entangled and a blue region where not. As we can see the measurement (blue curve) is never reaching the bound and is getting further away

from the entanglement region as N continues to increase. This is not surprising as γ decay will rapidly suppress entanglement when increasing the number of atoms. This is not a different result than the one in the superradiant regime of Fig. 5, where without single-photon detections no entanglement is confirmed due to the mixing of states during the evolution, but now is also increased by the γ contribution.

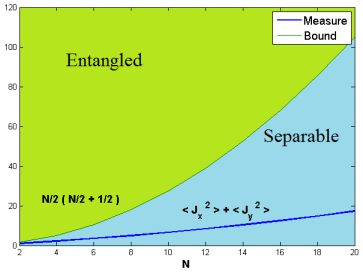

Figure 7. The scaling of the entanglement measure (blue curve) with the number of atoms N is computed for $\Gamma_{1D}/\gamma = 0.1$. The plot shows the optimal measurement value during all times t of the evolution. The green curve show the bound above which the state is confirmed to be entangled, separating in this way the two regions of the plot: a region where the state is confirmed to be entangled (green region) and a region where not (blue region).

4. Conclusions and outlook

We have shown that although unconditional collective decay does not produce entanglement, the situation improves dramatically (by $\sqrt{N}$) by employing high-efficiency photon detection, and it is possible to engineer genuine multipartite entangled Dicke states for up to $N \sim 10$ atoms.

Nevertheless, the spontaneous decay into free space is not generating entanglement and thus, increasing the difficulty for entangled states to appear, and in this case, a recent and promising theoretical approach to simulate open quantum systems in the SU(4) Lie Group representation [7] is used.

Further exploration from this system would be, first of all, to implement single-photon detections in the waveguide when spontaneous decay to free space is present $\gamma > 0$, and up to which extend in terms of number of atoms N, Purcell Factor Γ_{1D}/γ and detector efficiency η is possible to experimentally confirm entanglement. Another research could be to study the effect of coupling a tunable pump laser to the waveguide, in order to make favourable populating interesting states, like the $|0,0\rangle$ state in case of even N, which for $N = 2$ atoms is a singlet state. Other sudies can be done adapting this new SU(4) technique to calculate other interesting observables, for example, for photon statistics of the emitted light. Also one can use this simulation technique to simulate similar two-channel decay processes with large system size.

References

[1] Kimble H J 2008 *Nature* **453** 1023–30
[2] Vetsch E, Reitz D, Sagué G, Schmidt R, Dawkins S T and Rauschenbeutel A 2010 *Phys. Rev. Lett.* **104** 203603
[3] Goban A, Choi K S, Alton D J, Ding D, Lacroûte C, Pototschnig M, Thiele T, Stern N P and Kimble H J 2012 arXiv:1203.5108
[4] Hammerer K, Sørensen A S and Polzik E S 2010 *Rev. Mod. Phys.* **82** 1041–93
[5] Chang D E, Jiang L, Gorshkov A V and Kimble H J 2012 *New Journal of Physics* **14** 063003
[6] Chang D E, Cirac J I, Kimble H J 2013 *Phys. Rev. Lett.* **110** 113606
[7] Minghui Xu, Tieri D A and Holland M J 2013 arXiv:1302.6284
[8] Dicke R H 1954 *Phys. Rev.* **93** 99
[9] Gross M and Haroche S 1982 *Physics Reports* **5** 301–396
[10] Lee C T 1976 *Phys. Rev. A* **13** 4
[11] Stockton J K, Geremia J M, Doherty A C and Mabuchi H 2003 *Phys. Rev. A* **67** 022112
[12] Campbell S, Tame M S and Paternostro M 2009 *New Journal of Physics* **11** 073039
[13] Koashi M, Buzek V and Imoto N 2000 *Phys. Rev. A* **62** 050302
[14] Géza Tóth 2006 *J. Opt. Soc. Am. B* **24** 2
[15] Duan L -M and Kimble H J 2003 *Phys. Rev. Lett.* **90** 25